Influence of Spatial Resolution on Diurnal Variability during the North American Monsoon

J. LI AND S. SOROOSHIAN

CHRS, Department of Civil and Environmental Engineering, University of California, Irvine, Irvine, California

W. HIGGINS

Climate Prediction Center, NOAA/NWS/NCEP, Washington, D.C.

X. GAO, B. IMAM, AND K. HSU

CHRS, Department of Civil and Environmental Engineering, University of California, Irvine, Irvine, California

(Manuscript received 2 May 2007, in final form 18 April 2008)

ABSTRACT

Diurnal variability is an important yet poorly understood aspect of the warm-season precipitation regime over southwestern North America. In an effort to improve its understanding, diurnal variability is investigated numerically using the fifth-generation Pennsylvania State University (PSU)–NCAR Mesoscale Model (MM5). The goal herein is to determine the possible influence of spatial resolution on the diurnal cycle.

The model is initialized every 48 h using the operational NCEP Eta Model 212 grid (40 km) model analysis. Model simulations are carried out at horizontal resolutions of both 9 and 3 km. Overall, the model reproduces the basic features of the diurnal cycle of rainfall over the core monsoon region of northwestern Mexico and the southwestern United States. In particular, the model captures the diurnal amplitude and phase, with heavier rainfall at high elevations along the Sierra Madre Occidental in the early afternoon that shifts to lower elevations along the west slopes in the evening. A comparison to observations (gauge and radar data) shows that the high-resolution (3 km) model generates better rainfall distributions on time scales from monthly to hourly than the coarse-resolution (9 km) model, especially along the west slopes of the Sierra Madre Occidental. The model has difficulty with nighttime rainfall along the slopes, over the Gulf of California, and over Arizona.

A comparison of surface wind data from three NCAR Integrated Sounding System (ISS) stations and the Quick Scatterometer (QuikSCAT) to the model reveals a low bias in the strength of the Gulf of California low-level jet, even at high resolution. The model results indicate that outflow from convection over northwestern Mexico can modulate the low-level jet, though the extent to which these relationships occur in nature was not investigated.

1. Introduction

The North American monsoon (NAM) accounts for approximately 40%–80% of the annual rainfall in the southwestern United States and Mexico (Douglas et al. 1993; Stensrud et al. 1995). As a consequence, it has a tremendous influence on the summer weather, climate, and water resources of this region. The NAM is characterized by numerous multiscale interactions, both in space and time. The climatological and synoptic features of the NAM have been studied systematically at the continental and regional scales (see the reviews of Douglas et al. 1993; Adams and Comrie 1997; Higgins et al. 1997; Barlow et al. 1998), with renewed interest during the recent North American Monsoon Experiment (NAME) 2004 field campaign (Higgins and Gochis 2007). Because of the limitations in the observation network (Gochis et al. 2004) and in the capabilities of model physical parameterizations, many aspects of the NAM remain poorly understood, including the variability of local circulations, such as the land–sea

Corresponding author address: Soroosh Sorooshian, CHRS, Department of Civil and Environmental Engineering, University of California, Irvine, Irvine, CA 92697-2175.
E-mail: soroosh@uci.edu

DOI: 10.1175/2008JCLI2022.1

breeze and mountain–valley circulation, and the modulation of convection by complex terrain (Higgins and Gochis 2007; Higgins et al. 2006). The diurnal cycle of rainfall is one of these features.

In their landmark study, Negri et al. (1993, 1994) first identified the diurnal cycle of rainfall along the western coast of Mexico using satellite rainfall estimates. They found that convective storms occurred offshore during the early morning hours, with several local maxima around concave-shaped areas of the coastline. During the afternoon and evening, deep convection was most intense over land, with marked maxima along the western slopes of the Sierra Madre Occidental (SMO). Using high spatial and temporal resolution rainfall estimates from satellite, Sorooshian et al. (2002) both validated the findings of Negri et al. and documented inverse diurnal rainfall patterns between the Isthmus and the Gulf of Tehuantepec, as well as between the southern Mexican coastal area and offshore in the eastern Pacific. Although remotely sensed rainfall data provide unprecedented, integrated patterns of global precipitation, many studies (e.g., Garreaud and Wallace 1997) have noted that deficiencies of satellite rainfall estimation, namely, indirect rainfall estimation and limited rainfall sampling in space and time, can affect the accuracy of the results. For example, Berbery (2001) analyzed 3 yr of precipitation data from the National Centers for Environmental Prediction (NCEP) Eta Model (48-km horizontal resolution) and found that diurnal variations over the SMO were weaker than the satellite estimates. He argued that these differences were reasonable because the satellite rainfall estimates were based on the maximum instantaneous rainfall in the afternoon, while the model forecast was integrated over time.

The arguments above motivate the need for high spatial and temporal resolution ground-based observations to validate both modeled and satellite-retrieved precipitation. In the absence of high-resolution in situ data, we can use high-resolution numerical models to examine unresolved features of the diurnal variability. Coarse-resolution global models cannot resolve either the Gulf of California (GOC; e.g., Berbery 2001; Mo et al. 2005), which is a primary channel for moisture into southwestern North America (e.g., Stensrud et al. 1995), or the complex terrain of the region. On the other hand, high-resolution mesoscale models have been used to investigate the diurnal cycle with some success. Stensrud et al. (1995) reproduced the observed convective diurnal variations over the western slopes of the SMO using the fifth-generation Pennsylvania State University–National Center for Atmospheric Research (PSU–NCAR) Mesoscale Model (MM5) at a horizontal resolution of 25 km. From a comparison to observations gathered during the Southwest Area Monsoon Project (SWAMP), they found that the model overestimated convective precipitation frequencies over mountainous areas and had difficulty with the temporal phase in some regions. More recently, Gochis et al. (2002) examined the effect of the model convective parameterization scheme (CPS) on the diurnal cycle of rainfall over the SMO. They found that the time of peak rainfall intensity depended vitally on the CPS. Mo and Juang (2003) used the NCEP Regional Spectral Model at a horizontal resolution of 30 km to examine the influence of SST in the GOC on diurnal variations of precipitation within the NAM region. Li et al. (2004) investigated diurnal variations of rainfall over southwestern North America, and found that the model (i.e., MM5) did reasonably well with the diurnal cycle of precipitation over western Mexico, but not so well over Arizona (especially central Arizona) and northern Texas. None of the modeling studies to date have been able to reproduce the multiscale phase propagation of the diurnal cycle seen in observations, such as those from NAME.

Another and equally important feature is the GOC low-level jet (LLJ), which typically develops along the Gulf of California and typically reaches peak intensity in the early morning. The jet has been investigated using observations from SWAMP (e.g., Douglas and Li 1996); Douglas et al. 1998) and using numerical simulations (e.g., Stensrud et al. 1995, 1997; Anderson et al. 2001; Fawcett et al. 2002; Gochis et al. 2002; Li et al. 2004; Saleeby and Cotton 2004; Mo et al. 2005; Gao et al. 2007). In general, current models and analysis streams [such as the North American Regional Reanalysis (NARR) of Mesinger et al. (2006)] have difficulty with the amplitude, location, and diurnal phasing of the jet. Enhanced observations and higher-resolution models are needed to resolve mesoscale features of the NAM, including the LLJ, the land–sea breeze, and the mountain–valley circulations (Gochis et al. 2002; Li et al. 2004; Saleeby and Cotton 2004; Gao et al. 2007; Mo et al. 2005; Anderson et al. 2001; Berbery 2001). Collectively, these studies indicate that the physical parameterizations in the current generation of global and regional models needs additional improvements, that an increased model resolution will help, and that enhanced observations (such as those from NAME) are needed for model validation.

In a special issue of the *Journal of Climate* (2008, Vol. 20, No. 9) on NAME, Higgins and Gochis (2007) highlighted the following specific areas where NAME data

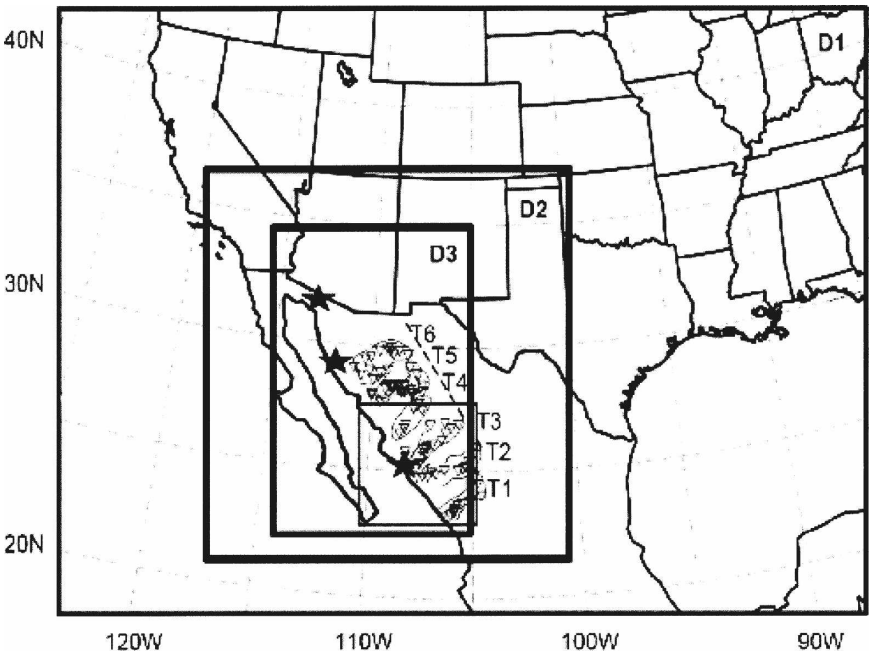

FIG. 1. Model domains for different tests: D1 (27-km horizontal resolution), D2 (9-km horizontal resolution), and D3 (3-km horizontal resolution). Triangles represent NERN locations. The western slope of the SMO is the area between the dashed line in D3 and the eastern coastline of the Gulf of California. The small box shows radar coverage (addressed in the text). The stars represent sounding locations, including operational sounding and the ISS radiosonde, during the NAME intensive observation period (IOP). From north to south, the stars show Puerto Penasco (ISS2), Kino Bay (ISS3), and Los Mochis (ISS4). T1–T6 are the six transects (discussed in text).

are contributing to improved understanding and more realistic simulation of the NAM:

- the frequency, intensity, temporal phase, and elevation dependence of the diurnal cycle of precipitation (Gochis et al. 2004, 2007);
- the spatial distribution of precipitation (Gochis et al. 2004, 2007; Lang et al. 2007); Gebremichael et al. (2007); Vivoni et al. 2007);
- the diurnal evolution and spatial distribution of the GOC LLJ (Johnson et al. 2007);
- the structure of observed stratiform precipitation around the NAM domain (Johnson et al. 2007; Lang et al. 2007); and
- the role of the land surface as a spatially heterogeneous assimilator of atmospheric processes (Vivoni et al. 2007).

In this manuscript, we investigate the effects of model resolution on the ability of the MM5 to capture some of these features, including diurnal variations of the LLJ over the northern GOC and localized rainfall features over the SMO. Several of the NAME 2004 datasets, including those from the NCAR Integrated Sounding Systems (ISS), NAME Event Rain Gauge Network (NERN), and NAME radar network will be used to validate the results. Attempts are made to identify possible physical mechanisms as a step toward understanding weaknesses in the model.

2. Numerical modeling

a. Study domain

To examine rainfall variability at different horizontal resolutions, the following two tests were designed:

- Test 1: Three nested domains (D1, D2, D3) were used in the simulations (see Fig. 1) with 27-, 9-, and 3-km horizontal meshes, respectively.
- Test 2: Same as test 1, except that only D1 and D2 are used.

b. Model physics

MM5 was employed; it provides multiple options and schemes to represent a variety of physical processes. Consistent with the results of Gochis et al. (2002), the Grell (1993) CPS was used in domains 1 and 2 (only). Additional model physics schemes selected for the study include explicit cloud microphysics (Tao and Simpson 1989), Medium-Range Forecast (MRF) boundary layer scheme (Hong and Pan 1996), and the Noah land surface model (Chen and Dudhia 2001). The

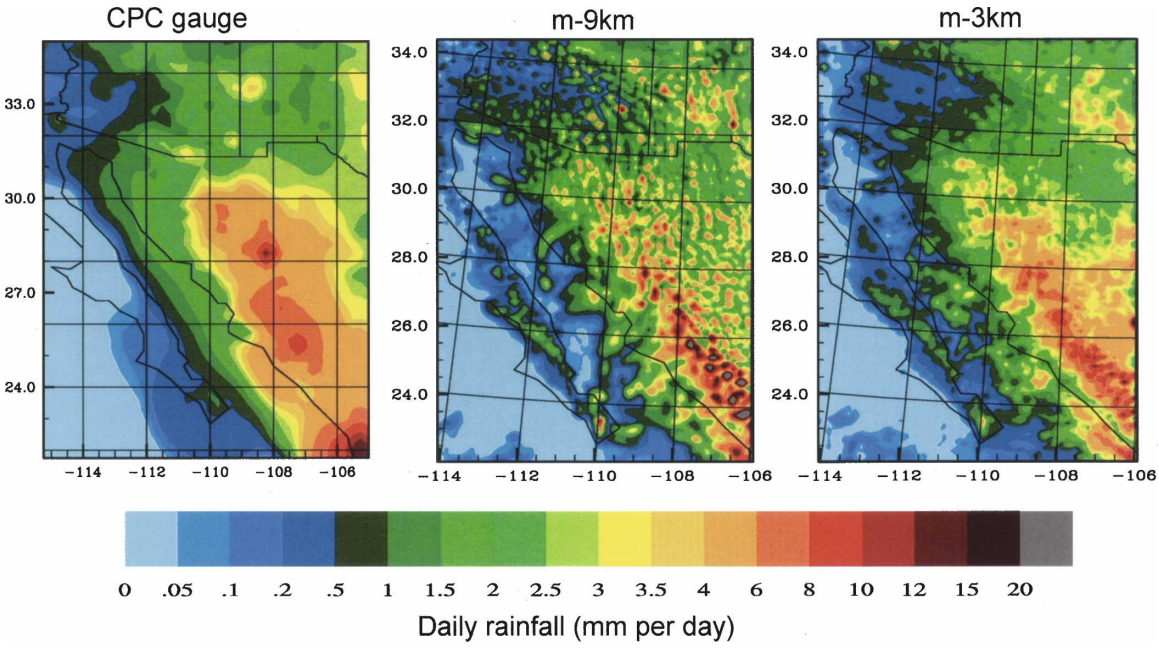

FIG. 2. Mean rainfall over the core monsoon region from model results with 9-km resolution (m-9km), 3-km resolution (m-3km), and CPC gauge gridded data during the simulation time.

vertical coordinate of MM5 is a terrain-following coordinate system. In this study, 31 vertical sigma layers were employed from the surface to the top of atmosphere at 100 mb.

The operational NCEP Eta Model 212 grid (40 km) model analysis data for July and August 2004 were used as forcing fields. The Eta Model analysis data were used as model initial conditions and model boundary conditions in all tests. The model was initialized at 0000 UTC and integrated up to 48 h. The authors also tried to use NARR (Mesinger et al. 2006) data as the initial and boundary conditions, but these tests were less successful than those presented here.

c. *Observation data*

To evaluate the model results, the following "independent" datasets were used:

(i) Climate Prediction Center (CPC) 0.25° unified rain gauge daily precipitation analysis for the United States and Mexico (available online at http://www.cpc.ncep.noaa.gov/products/precip; see also Higgins et al. 1999),
(ii) NAME 2004 radar data along the GOC (Lang et al. 2007),
(iii) NERN hourly data from 85 gauges installed in clusters at six transects (see Fig. 1; Gochis et al. 2004), and
(iv) NCAR ISS radiosonde data at Puerto Penasco (ISS2), Kino Bay (ISS3), and Los Mochis (ISS4) for 3 July–15 August 2004 (data were available 4 times per day).

3. Results

a. *Monthly mean rainfall*

A comparison of the mean daily rainfall in observations and in the model for July–August 2004 (Fig. 2) shows that higher spatial resolution improves the distribution and intensity of rainfall. The high degree of heterogeneity in the rainfall patterns for the 9-km resolution is strongly correlated with the topography. Therefore, the unrealistically large rainfall amounts (>20 mm) over the hills along the SMO can be attributed to the degree of coarseness of the resolution (9 km). We note that at coarser resolution the model also overestimates precipitation, especially over the southern SMO. Stensrud et al. (1995) suggested that this model deficiency may be due to "both the complexities of using multiple grids with different CPSs and the convective trigger function."

b. *Diurnal cycle of rainfall*

1) RAINFALL DIURNAL VARIATION OVER THE SOUTHWEST UNITED STATES

The mean 6-h precipitation accumulation (Fig. 3) shows that the model, irrespective of resolution, generates rainfall over mountainous areas that are generally comparable to stage II radar–gauge merged rainfall

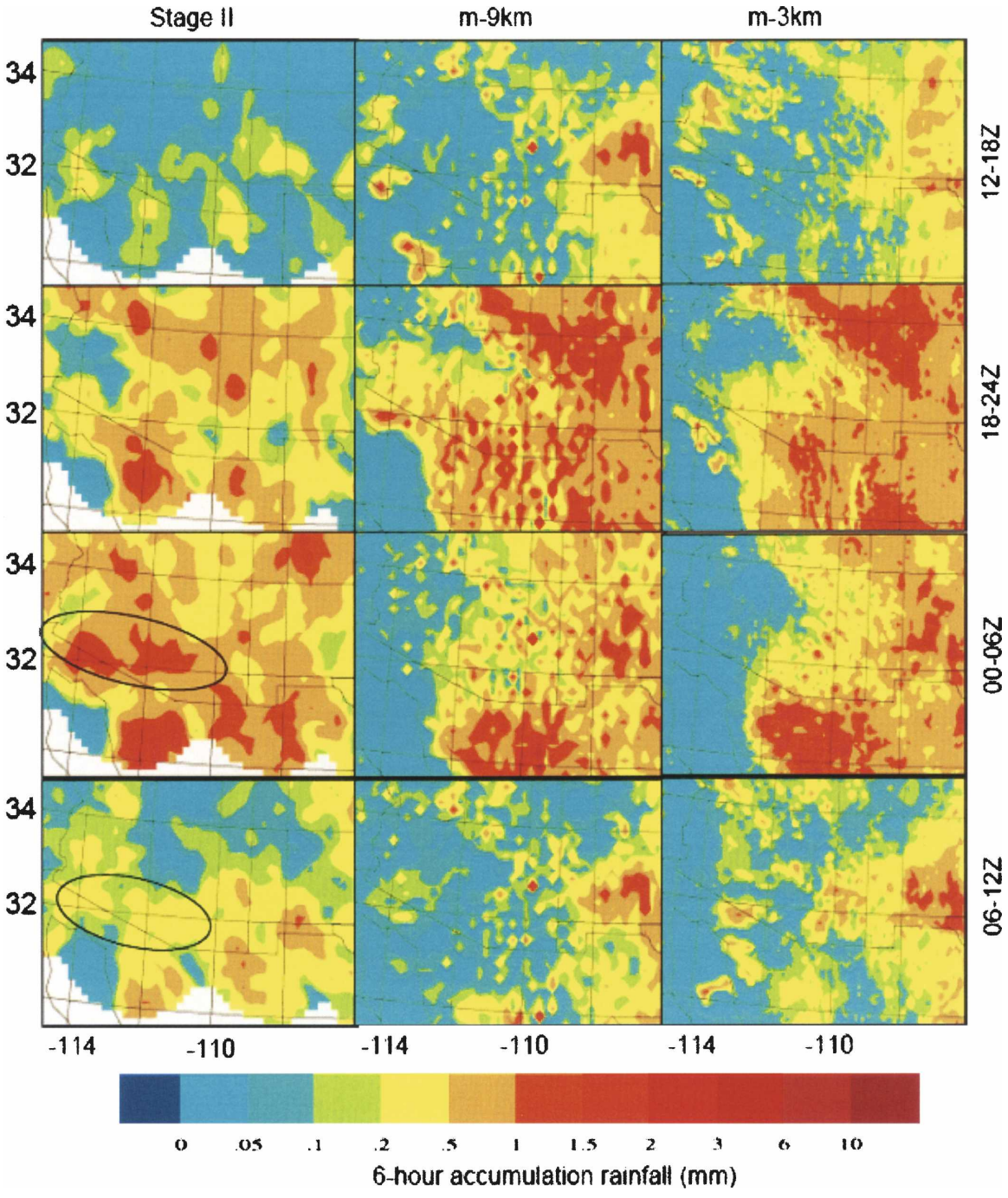

FIG. 3. Mean 6-h rainfall accumulation comparison between stage II radar, gauge mixing data, and model results at different resolutions over northern Mexico and southern Arizona during the simulation time.

data. A closer examination reveals some significant differences, especially in the evening and early morning hours, including over the southwestern United States. A possible explanation for this may be that the model underestimates the low-level meteorological fields over the northern Gulf of California, and in particular the southerly winds (details will be discussed later).

2) DIURNAL CYCLE OVER THE WESTERN SLOPES OF THE SMO

NAME radar observations at two locations over the west slope of the southern SMO (Lang et al. 2007) were used for this study. In particular, continuous radar data from 9 to 22 July and from 10 to 18 August (a total of

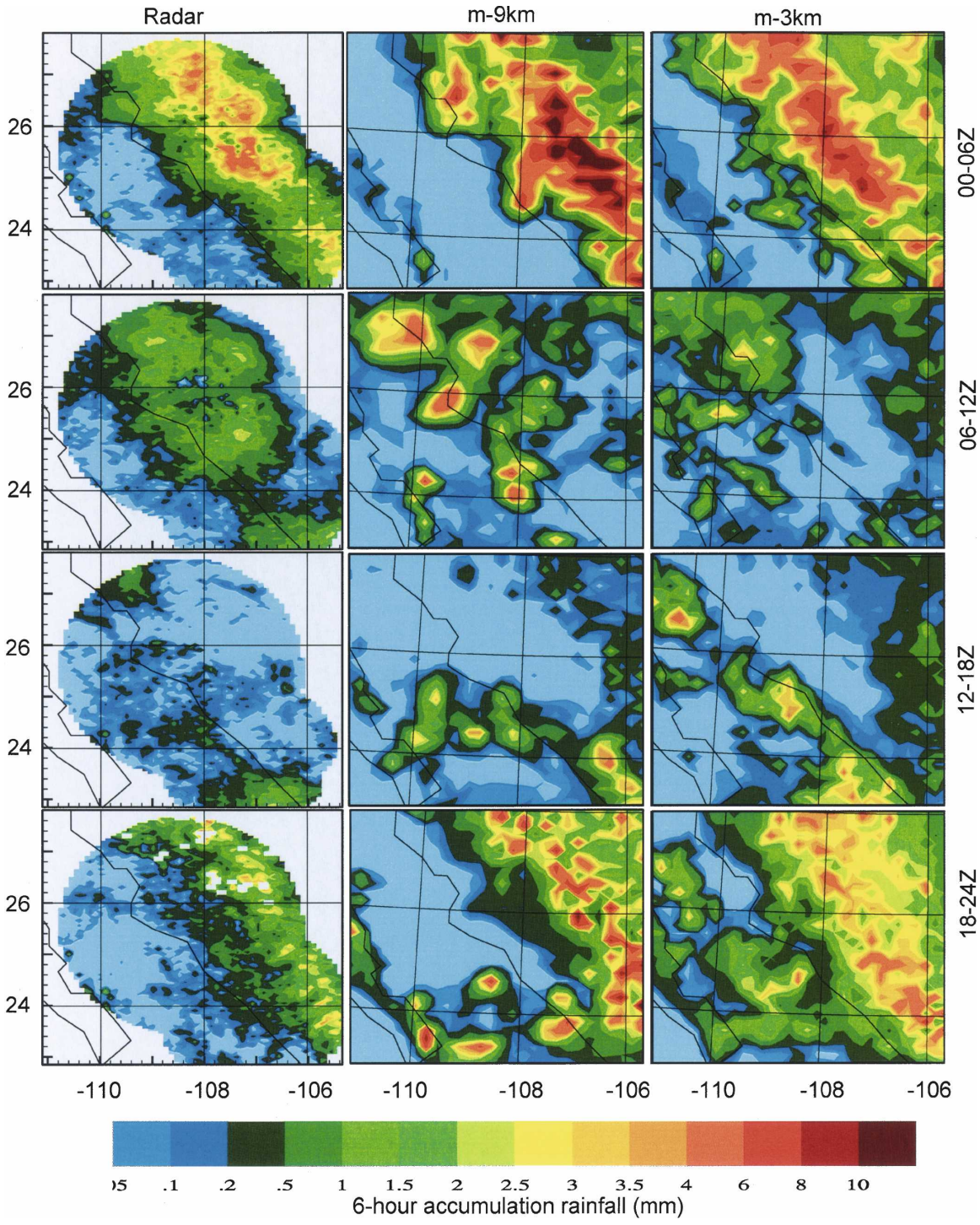

FIG. 4. The 6-hourly mean rainfall comparison between radar data and model output at different resolutions during 9–22 Jul and 10–18 Aug 2004.

23 days) were employed. A comparison (see Fig. 4) of 6-hourly accumulated mean rainfall shows that the model exhibits patterns that are similar to radar, both in time and in space, with maximum rainfall from 0000 to 0600 UTC. Note, however, that the model overestimates rainfall from 1800 to 0600 UTC at both resolutions, indicating that convection initiates too early in the day in the model, irrespective of horizontal resolution. Alternately, the model underestimates rainfall during the early morning hours (0600–1200 UTC).

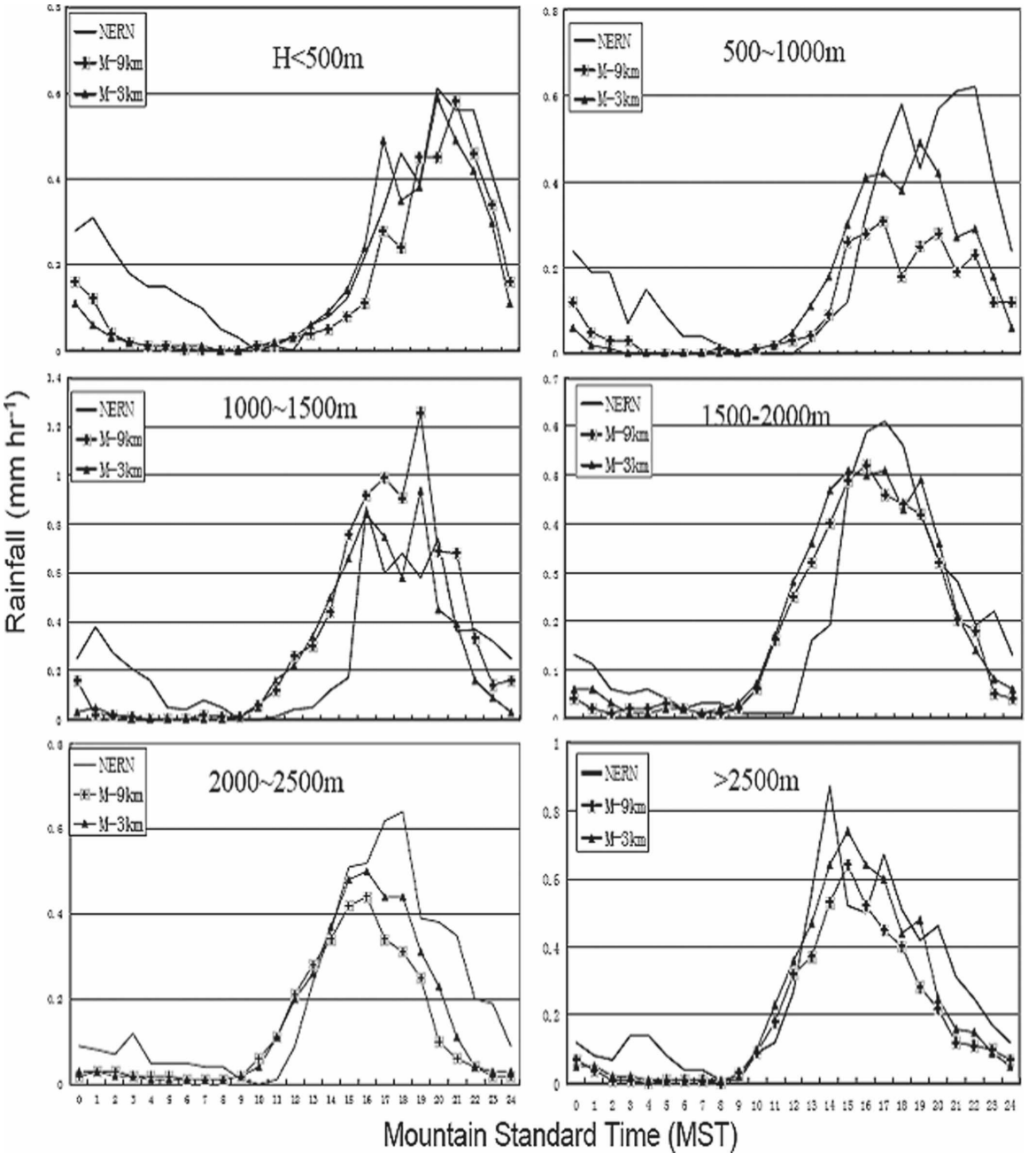

FIG. 5. Comparison of mean diurnal variation in rainfall between NERN data and the model output at different resolutions over specific terrain elevation ranges during the simulation time.

Generally, the MM5 reproduces the rainfall patterns with greater fidelity over the northern GOC.

A comparison of the mean diurnal cycle of rainfall from the NERN and the model for different elevation bands (Fig. 5) shows that the higher resolution is somewhat better than the lower resolution, independent of elevation. Specifically, the higher-resolution model generates larger rainfall amounts from late afternoon to early evening than the coarse-resolution model. Again, the results show that precipitation begins earlier in the model than in the observations, independent of resolution, especially between 1000 and 2000 m. In addition, the model underestimates the NERN rainfall maxima above 1500 m.

Two additional conclusions can be drawn from Figs. 4 and 5. First, if the negative bias of NERN is considered (as discussed by Gochis et al. 2004), then the radar data underestimate the rainfall over the SMO. Second,

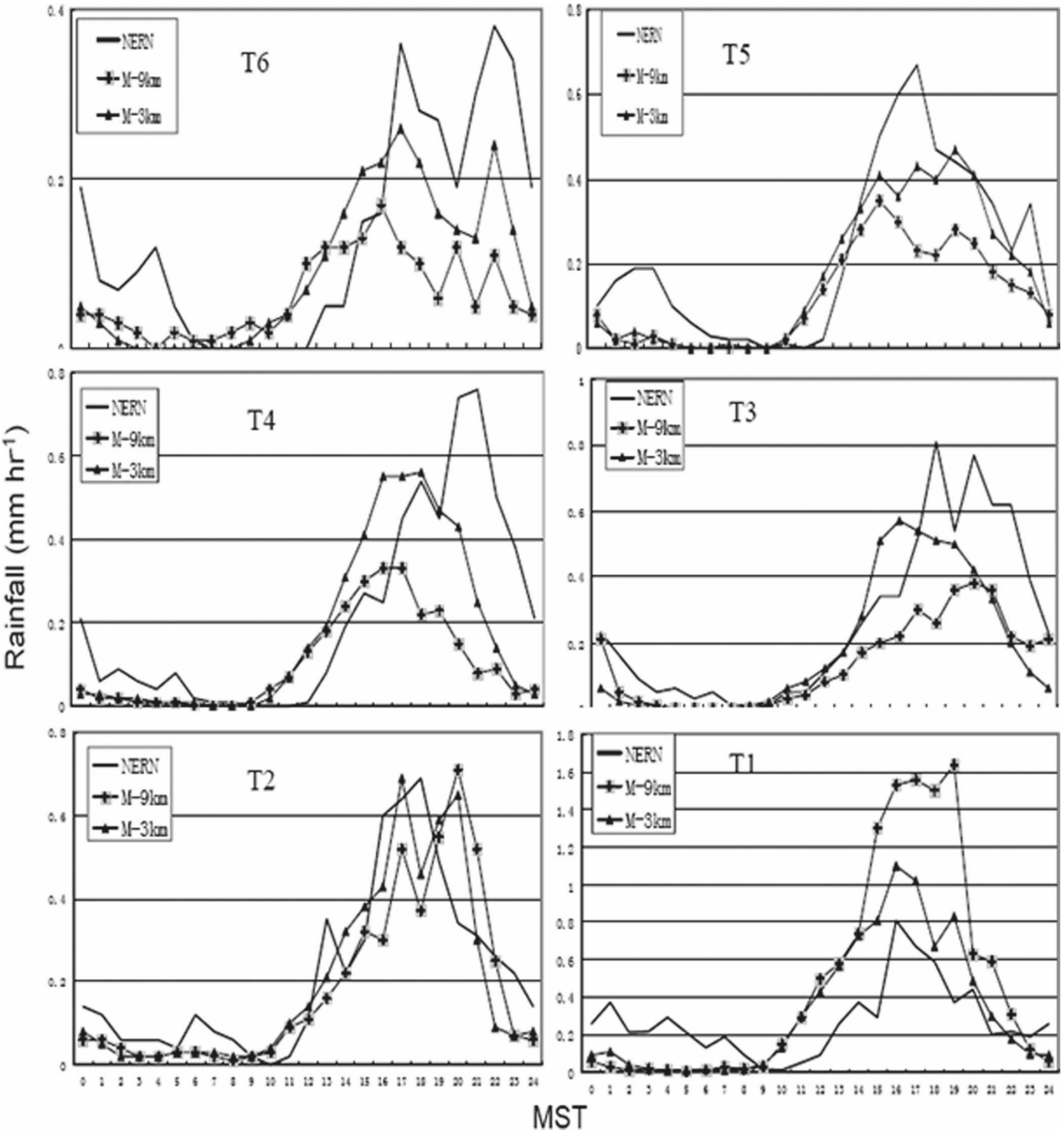

FIG. 6. As in Fig. 5, but over specific transects during the simulation time.

the model exhibits deficiencies in predicting rainfall amounts that occur from midnight to early morning. A comparison of the diurnal variation of rainfall from NERN and the model for each of the NERN transects (Fig. 6) clearly shows a noticeable improvement for the high-resolution model.

The primary conclusion that can be drawn from the above comparisons is that the rainfall distributions are similar for both horizontal resolutions, but the rainfall intensities through the diurnal cycle are better at a higher resolution. In what follows, we attempt to provide a physical explanation for this.

Generally, when the model resolution increases, the representation of subgrid-scale features (e.g., terrain and land cover) tends to improve. It is fair to conclude that if resolution matters, then there must be differences in model outcomes for the orographically forced vertical motion near the surface and the surface heating. With respect to the first issue (i.e., near-surface air vertical motion), Luo and Yanai (1983) provided a theoretical explanation in the Tibetan region and Ciesielski and Johnson (2008) used this framework in their study of the SMO region.

In this paper we suggest that the higher-resolution

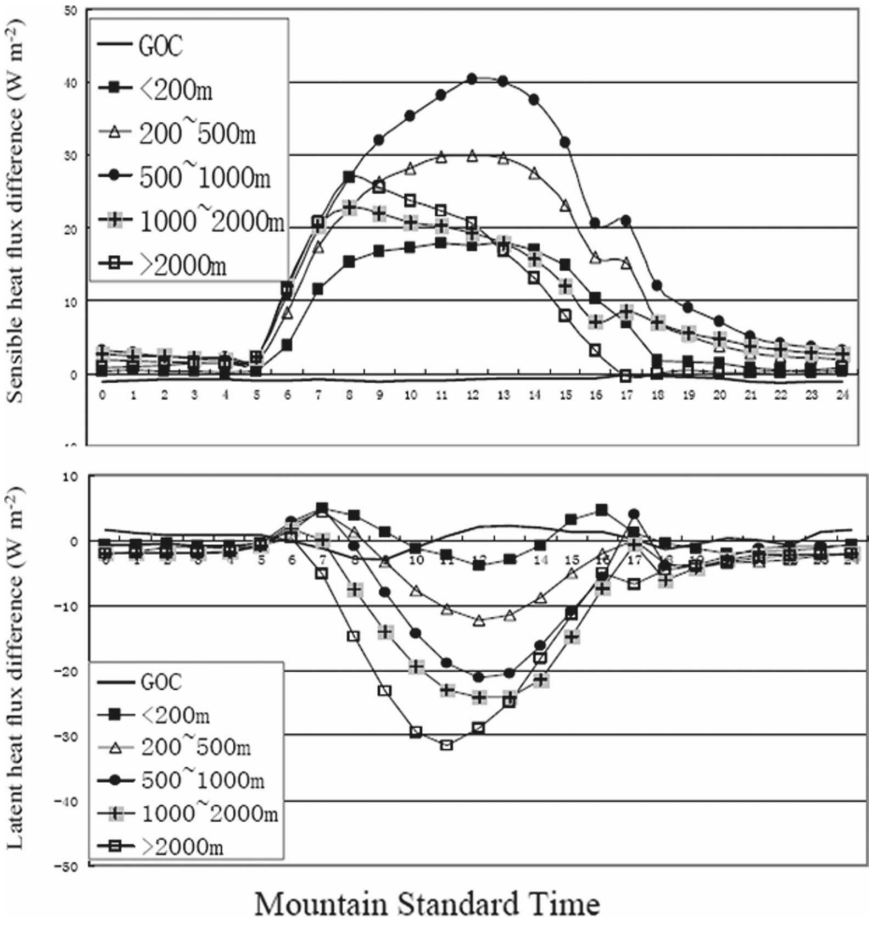

FIG. 7. (top) Mean surface sensible heat plus latent heat flux differences (W m^{-2}; model result from 9 km minus 3 km) at different elevation ranges when different resolutions are used. (bottom) Same as (top), but for PBL height differences (m).

model better captures the contribution of surface heating to the variations of the meteorological fields, such as convection. Diurnal variations of the difference in mean surface sensible heat flux (Fig. 7, top) and latent heat flux (Fig. 7, bottom) for different elevation ranges (expressed as the difference between the 9- and 3-km results) show that the primary differences occur during the daytime. The mean model sensible heat fluxes are 20–40 W m^{-2} higher at lower resolution, with the highest amounts occurring between 200 and 1000 m. On the other hand, the mean model latent heat fluxes at 3-km resolution are about 10–30 W m^{-2} lower at coarse resolution, with the largest differences over the region where elevation is greater than 500 m. These results indicate that model resolution could modulate the features of surface turbulent fluxes and then affect the convection development (e.g., latent heating processes not only transport the energy to the atmosphere but also water vapor). The results (Fig. 7) and rainfall diurnal variations (Figs. 2–6) suggest that higher resolution can better represent the distributions of surface sensible and latent heat fluxes.

The above analysis was intended to provide an overview of the effect of model resolution on capturing the rainfall variations. What follows next is an examination of the effect of the model resolution on the gulf surge, which is another important phenomenon during the monsoon season.

c. *Gulf surges*

We begin with an analysis of the ability of MM5 to simulate gulf surge events during NAME 2004. For the sake of brevity, we define surges as occurring when the daily temperature is greater than 22°C, daily dewpoint is greater than 18°C, and daily northward wind is greater than 5 m s^{-1} at Guaymas, Mexico. Based on these criteria, the model reproduced NAME 2004 surge events occurring on 13–14, 22–23, and 28–29 July, consistent with the events discussed in Johnson et al. (2007). For several of the other observed surge events

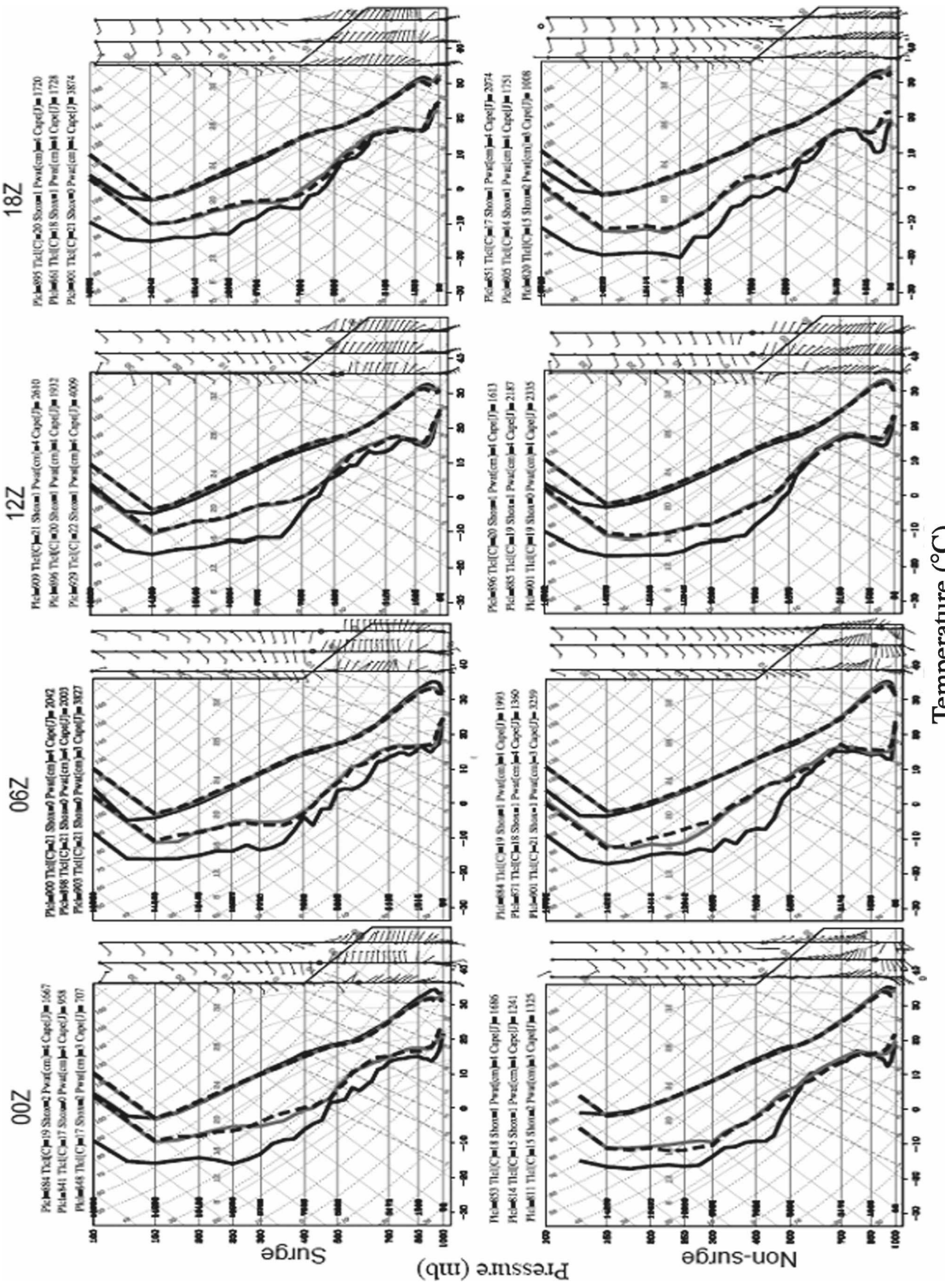

FIG. 8. (left page) Mean sounding comparisons between ISS observed data at Puerto Penasco and model results at the grid closest to the observation location during the observation period: observed (black solid lines), model at 9-km resolution (gray solid lines), and model at 3-km resolution (black dashed lines). The three-lines of text in each panel list pressure at LCL, temperature at LCL, the Showalter index, precipitable water, and CAPE for (from top to bottom) the model at 3- and 9-km resolutions, and observed. (right side of each panel, from left to right) The three column wind vectors represent observed, 9-, and 3-km resolution model winds. (right page) Same as (a), but for ISS4 at Los Mochis, Mexico.

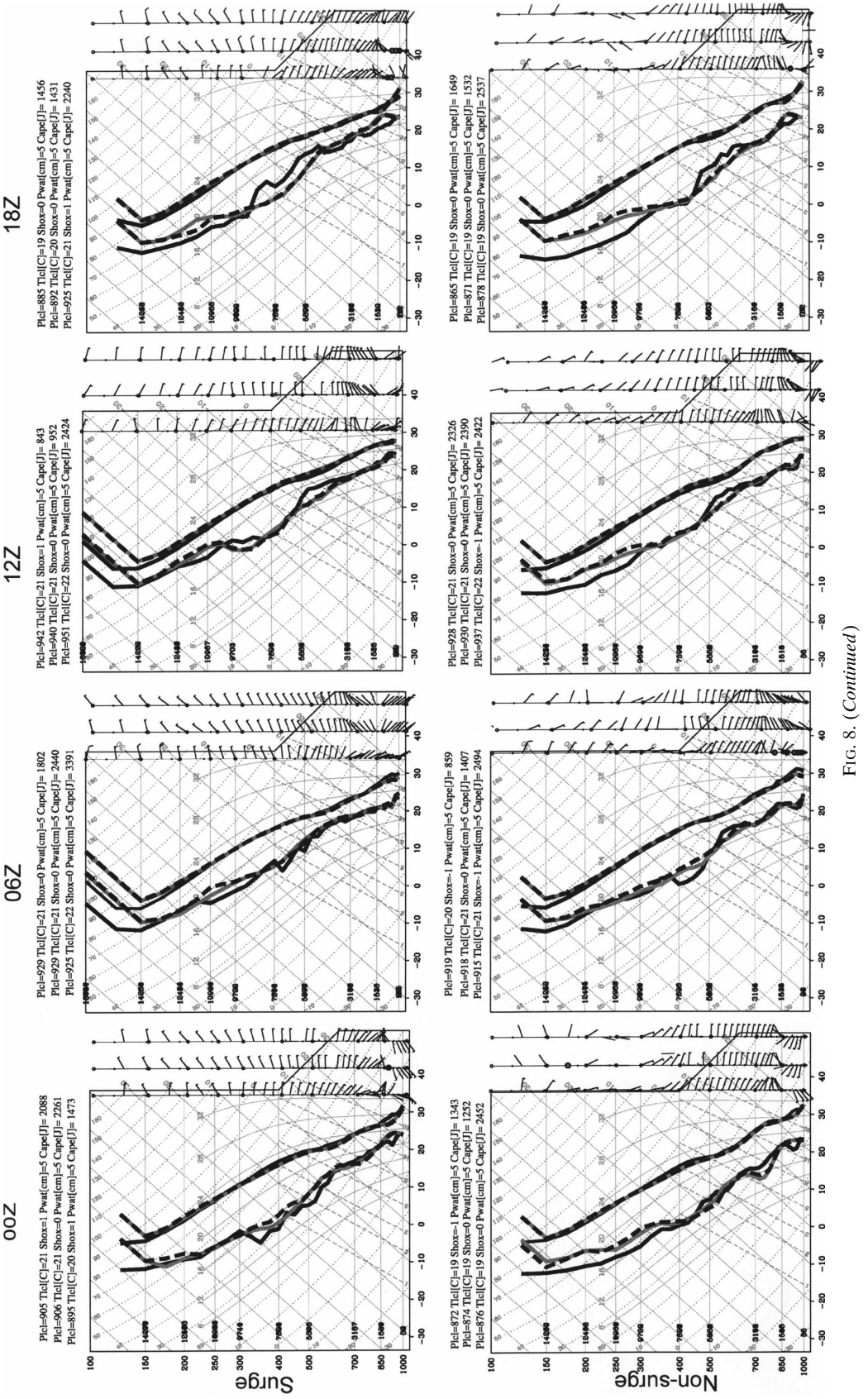

FIG. 8. (*Continued*)

(see Johnson et al. 2007 for details), the model generated weak wind (meridional winds less than 5 m s^{-1}) at both 3- and 9-km.

1) Comparison of ISS soundings with model simulations

Through checking the ISS observation based on the surge criteria mentioned above, a different number of the soundings that match between models and observations is found. For example, there were as many as 25 soundings at the Kino Bay location during nonsurge days at 1200 UTC, while only 7 soundings were measured at Los Mochis during surge days at 1800 UTC. The following comparisons are based on the matched samples at each case.

A comparison between available ISS data at Puerto Penasco, Mexico, and corresponding model results at the grid cell closest to the ISS (see Fig. 8a) shows that, for both surge and nonsurge periods at both resolutions, the model reproduces the observed vertical structure of meteorological variables, including low-level temperature, dewpoint, and wind shear with height. Both the model and observations indicate that the probabilities of convection are very low most of the time, except during surge periods. The model overestimated dewpoint temperatures below 950 mb (especially during nonsurge periods) and underestimated southerly winds below 850 mb. This deficiency affects the water vapor transport into Arizona. In addition, the model generated less CAPE at night and during the early morning (0600 and 1200 UTC), and more CAPE during the day (0000 and 1800 UTC) than in the observations.

A similar comparison was completed for the ISS located at Los Mochis, Mexico (Fig. 8b). In contrast to Puerto Penasco, the model generated a relatively good vertical profile of dewpoint temperatures. However, the model overestimated dewpoint temperatures at lower levels, especially at 0000 and 1800 UTC. At this location the model generated less CAPE than in the observations at all times of the day, except at 0000 UTC during surge periods, which means that the model underpredicts the likelihood of convection.

2) Comparison of low-level winds over the Gulf of California

A comparison of the low-level (from the surface to 700 mb) wind at Puerto Penasco during surge and nonsurge periods (Fig. 9) shows that the model reproduces the meridional component of the wind, though it is weaker than the observations, for both surge and nonsurge events. The model also captures the diurnal peak of the southerly winds for the surge events, but not for the nonsurge periods. However, this was not the case for the nonsurge period. Our results are consistent with previous investigations (e.g., Mo et al. 2005; Stensrud et al. 1997; Saleeby and Cotton 2004; Gao et al. 2007) that have documented the inability of models to reproduce the nighttime features of the GOC LLJ. The model results are largely independent of horizontal resolution in this case. Low-level winds were also examined at the remaining ISS locations. Once again, the results (not shown) indicated that the model underestimates the southerly winds during both surge and nonsurge periods.

A standard Student's t test was used to check for significant differences between the models and observations. The correlation coefficients between models at different resolutions and observations at each vertical layer (37 total vertical layers) had been calculated separately. Given a significance level α (= 0.05 in this study) and the statistical number N, the threshold Student's t-test value t_a is given from the t table. The threshold correlation coefficient r_c is then calculated as follows:

$$r_c = \sqrt{\frac{t_a^2}{N - 2 + t_a^2}}. \quad (1)$$

In this paper, r_c varies because of differences of the statistical number N (i.e., the N value depends on different cases, such as the time, and surge or nonsurge status). The results of r_c indicate that, most of the time, the differences between models and observations are statistically important.

A comparison of the mean simulated water vapor flux from the surface to 1000 m over the northern GOC at 0100 and 1300 UTC during surge periods (Fig. 10a) shows strong fluxes from water to land at 0100 UTC, consistent with previous results (e.g., Berbery 2001; Gochis et al. 2002; Fawcett et al. 2002; Li et al. 2004; Mo et al. 2005; Saleeby and Cotton 2004; Gao et al. 2007). At 1300 UTC, the water vapor fluxes are along the eastern GOC and the coastal lowland of western Mexico, again consistent with previous studies (e.g., Fawcett et al. 2002; Li et al. 2004; Anderson et al. 2001). The fluxes are relatively weak during the late afternoon at 9 compared to 3 km.

During nonsurge periods at 1300 UTC (not shown), the model generates weak northward water vapor flux over the northern GOC, which is much weaker than during the surge periods. During nonsurge periods at 0100 UTC (not shown), the model also generated flux from water to land, but it was relatively weak in comparison with surge periods.

A similar analysis at 0300, 0500, 0700, and 0900 UTC 13 July (Fig. 10b) shows that the model (at 3-km resolution) generates stronger low-level water vapor trans-

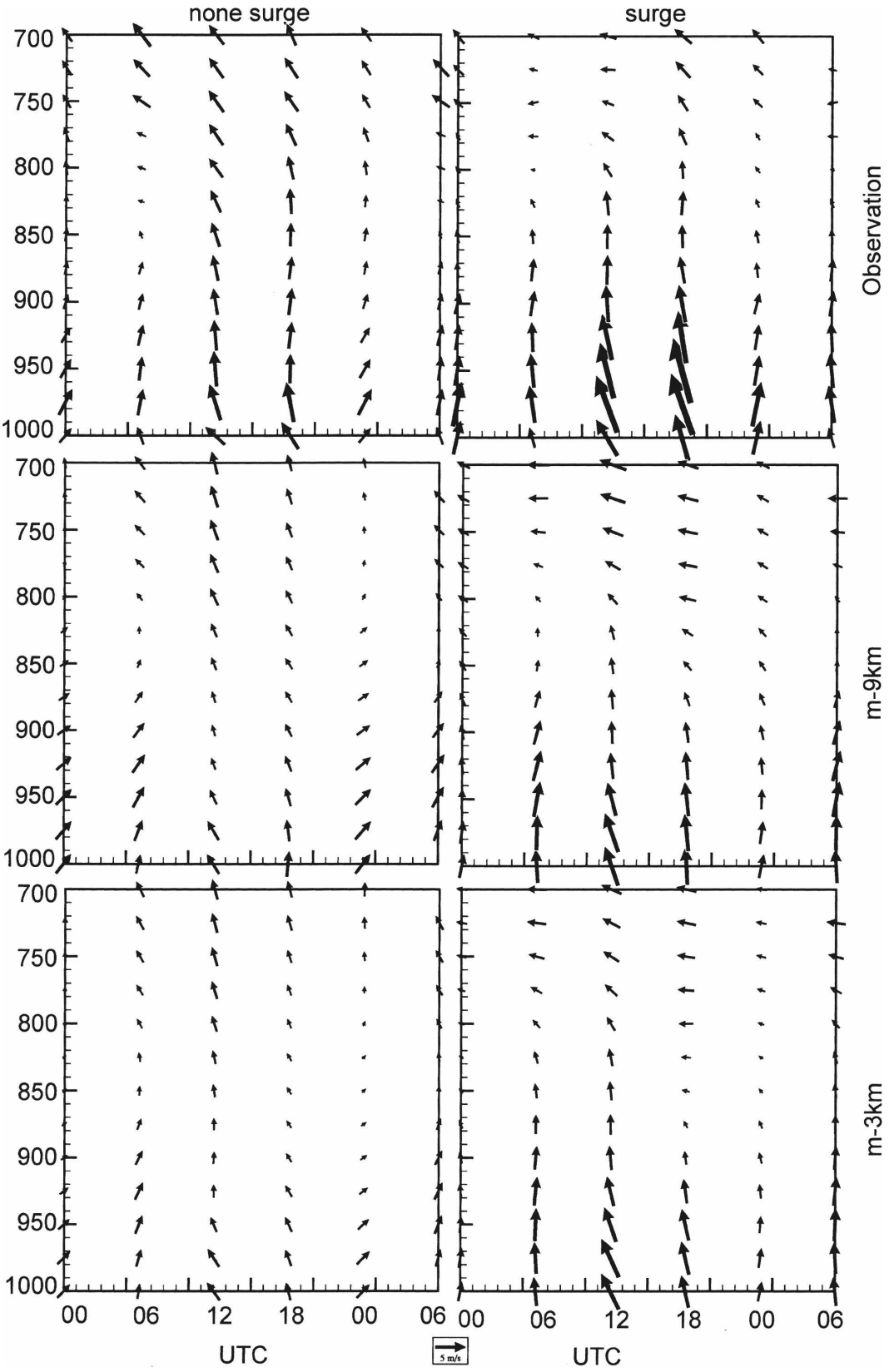

FIG. 9. The mean diurnal variation of wind vector at a low level (surface to 700 mb) between observations at ISS2 and model gridpoint results closest to the observation location during the observation period (~3 Jul–15 Aug 2004).

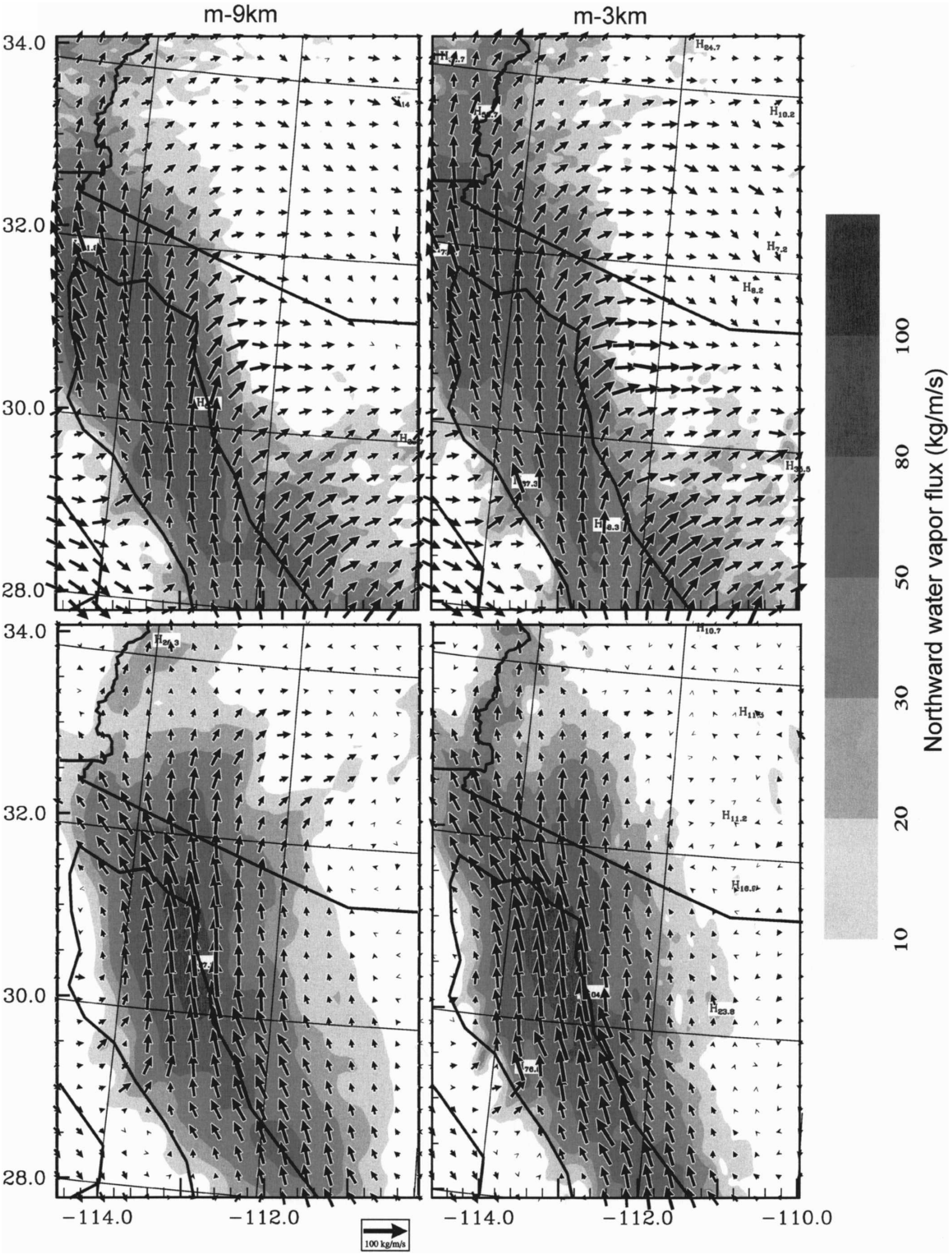

FIG. 10. Modeled water vapor flux over the northern Gulf of California at (left page) (top) 0100 and (bottom) 1300, and (right page) 0300, 0500, 0700 and 0900 13 Jul 2004 during the surge.

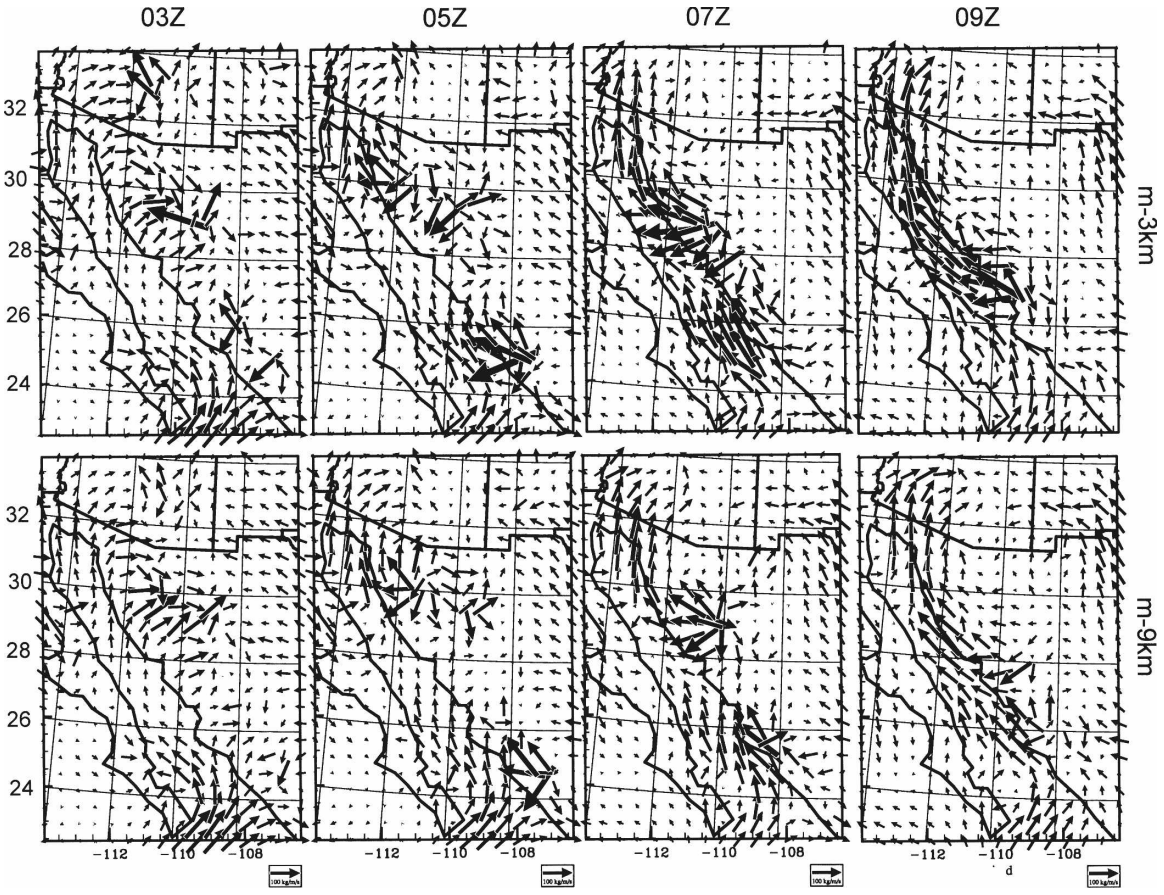

FIG. 10. (*Continued*)

port along the GOC and along the east coast of the GOC in this case. This may be because at 3-km resolution the model generates stronger convection, and thus stronger outflow, than the 9-km resolution. Fawcett et al. (2002) suggest that the easterly outflow is geostrophically accelerated to the north because of the east–west pressure gradient between the cool elevated slopes and the warmer free atmosphere to the west. Anderson et al. (2001) suggested that the pressure gradient is associated with nighttime slope cooling over the elevated SMO versus the warmer free atmosphere over the GOC. Our results (Figs. 10a,b) are consistent with their results, and so it is reasonable to conclude that the outflow from the convection that occurs on the west slope of the SMO results in the modulation of the intensity of the nighttime water vapor fluxes along the GOC and the coastal areas.

3) SURFACE WIND OVER THE GOC

A comparison of surface winds from the Quick Scatterometer (QuikSCAT), the Eta Model analysis, and the model at both horizontal resolutions for both surge and nonsurge periods (Fig. 11) shows that MM5 produced surface winds with similar magnitudes to those of QuickSCAT over the northern GOC, but winds were oriented roughly 90° out of phase along the central GOC during nonsurge periods. During surge periods, the Eta Model analysis exhibited stronger southerly wind than QuikSCAT and the model. Part of the explanation for MM5's deficient performance along the central GOC could be our choice of convective parameterization. Gochis et al. (2002) suggested that the Grell CPS could not generate surface winds as well as the Kain–Fritsch CPS, despite fact that the Grell CPS produces more accurate rainfall over western Mexico.

d. Case studies about the hourly rainfall evolution

1) CASE 1 (13–14 JULY)—SURGE PERIOD

Although the model generates a reasonably good rainfall distribution on monthly time scales, its performance at higher temporal resolutions is less accurate. For example, a comparison of hourly rainfall from the NAME radar data to the corresponding model data for

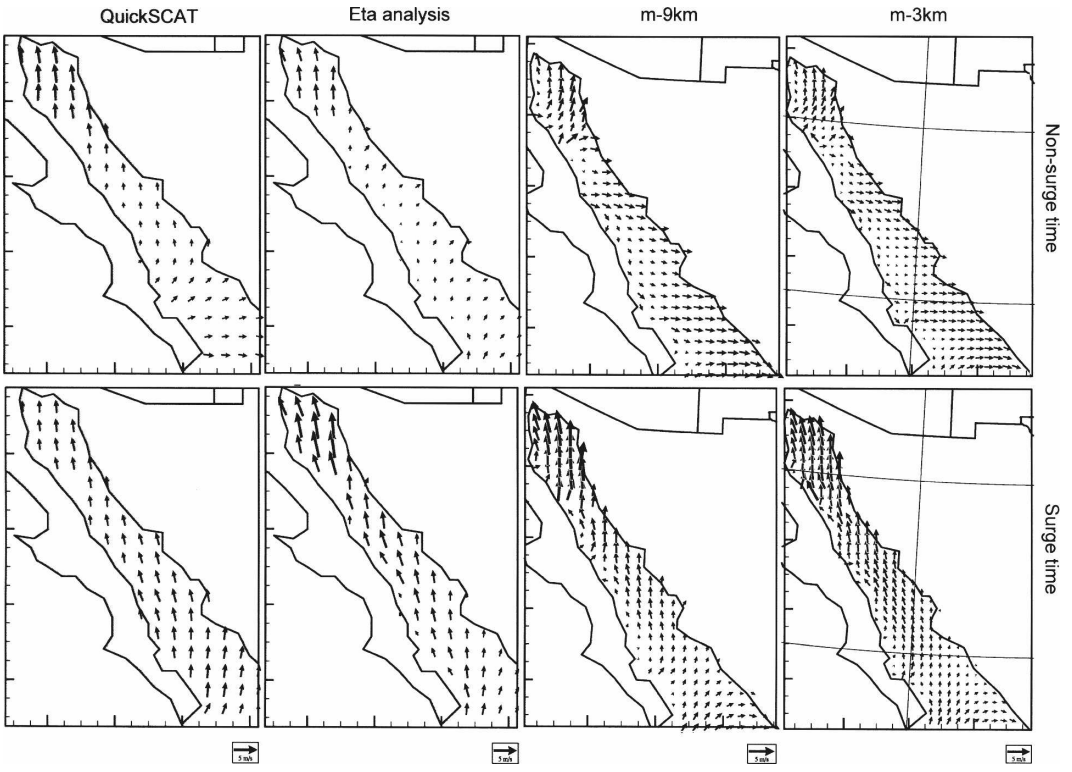

FIG. 11. Mean surface wind comparison between QuikSCAT, Eta Model analysis, and models with different resolutions during surge and nonsurge times.

the 13–14 July gulf surge event (Fig. 12) shows that during the first 3 h the model generates similar rainfall patterns as the radar for the 3-km resolution, but not the 9-km resolution. After 0400 UTC, the radar shows strong rainfall rates along the coastal region of the GOC while the model shows very weak rainfall rates, irrespective of resolution. This implies that the model can generate convective storms triggered by orography, but the model is unable to predict the nighttime convection that occurs over the lower-elevation coastal regions later in the day. As shown earlier (Fig. 8b), the model underestimates the CAPE in this region during surge periods.

The modeled vector wind and potential temperature for the 29th sigma layers (~0.9865) at 0300, 0500, 0700, and 0900 UTC 13 July 2004 (Fig. 13) show colder and stronger outflow for the high-resolution run. These results support the conclusions of previous studies that the model can reproduce upslope winds very well.

A comparison of the model-generated southerly winds at both resolutions at the grid point nearest ISS4 and the observation (see Table 1) indicates that the model at 3-km resolution slightly overestimated values and the model at 9-km resolution underestimated values near the ground surface.

Figure 13 also indicates that the convective outflow from the western slope of the SMO does contribute to modulation of the GOC LLJ, especially the outflow from the convective storms, which occur over northwestern Mexico. The outflow from the southern SMO can also reach the northern GOC if it is sufficiently strong.

A comparison of the vector wind and 200-hPa height from the Eta Model analysis to the model at 3-km resolution (Fig. 14) shows that generally the model reproduces the synoptic patterns. However, the model underestimates the 200-hPa heights. Also, there were the differences near the GOC between the two datasets, which could be one of the reasons that the model cannot reproduce the rainfall near the GOC areas. The results further indicate that the model has difficulty reproducing the atmospheric fields, not only at low levels, but also at high levels over the GOC areas. One of the reasons for this difference in Fig. 14 may be that the 100-mb level is not high enough to be selected as the model top layer, especially during the period when deep convection or strong synoptic system occurs.

2) CASE 2 (13 AUGUST)—NONSURGE PERIOD

Figure 15 is the hourly rainfall comparison from 0100 to 0600 UTC 13 August. The model generated the rain-

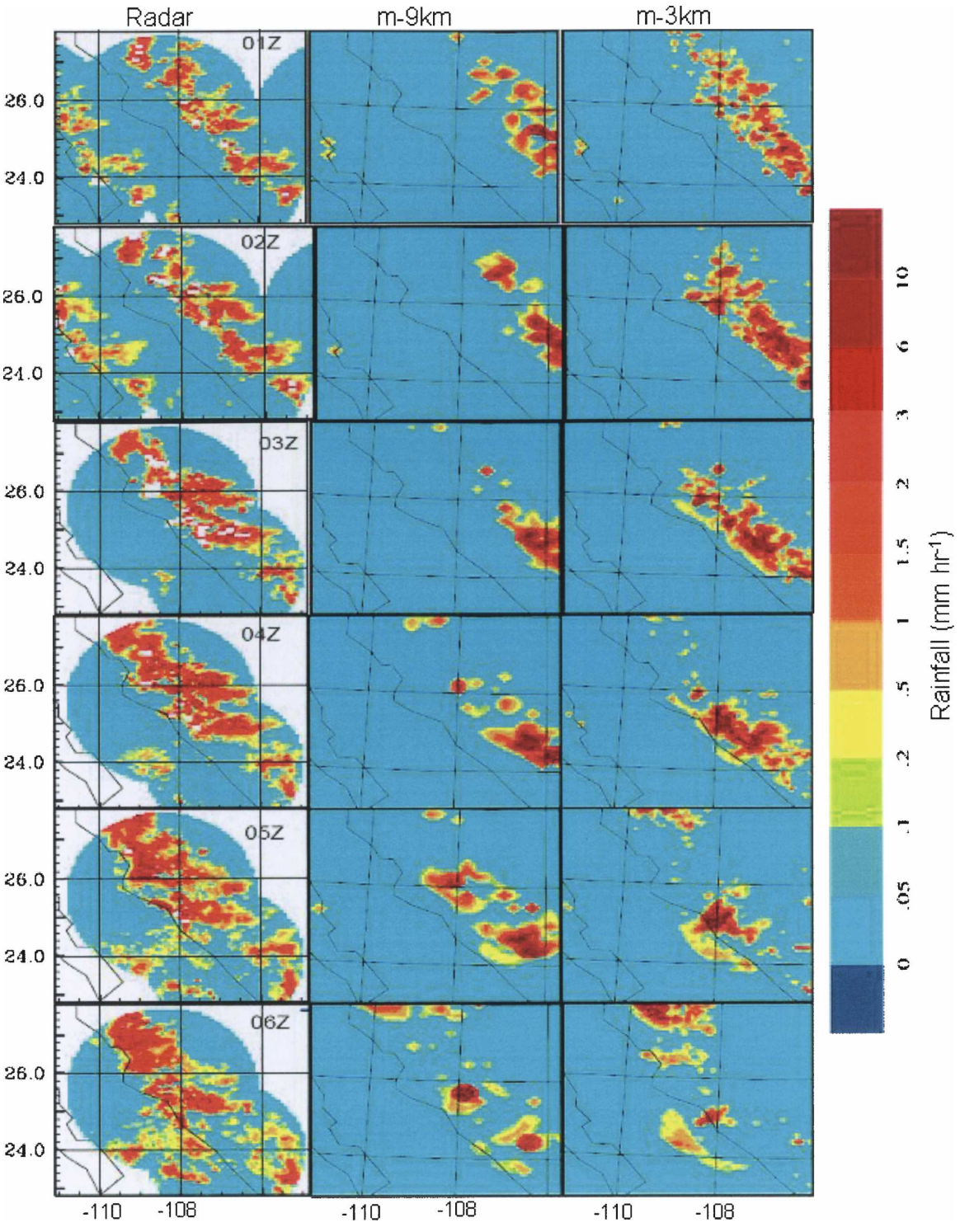

FIG. 12. Rainfall comparison between radar data and the models with different resolutions from 0100 to 0600 UTC 13 Jul 2004.

fall pattern very well from the late-afternoon to early evening hours. The results were especially improved for the 3-km resolution model over the high-elevation region. Again, the model (irrespective of resolution) cannot reproduce the nighttime rainfall over the low-elevation east coast of the GOC and the nearby slope. The analysis of the surface wind vector and potential temperature at 29 sigma levels indicates that the model surface outflow from the 3-km resolution is stronger than the 9-km case (not shown). In comparison with

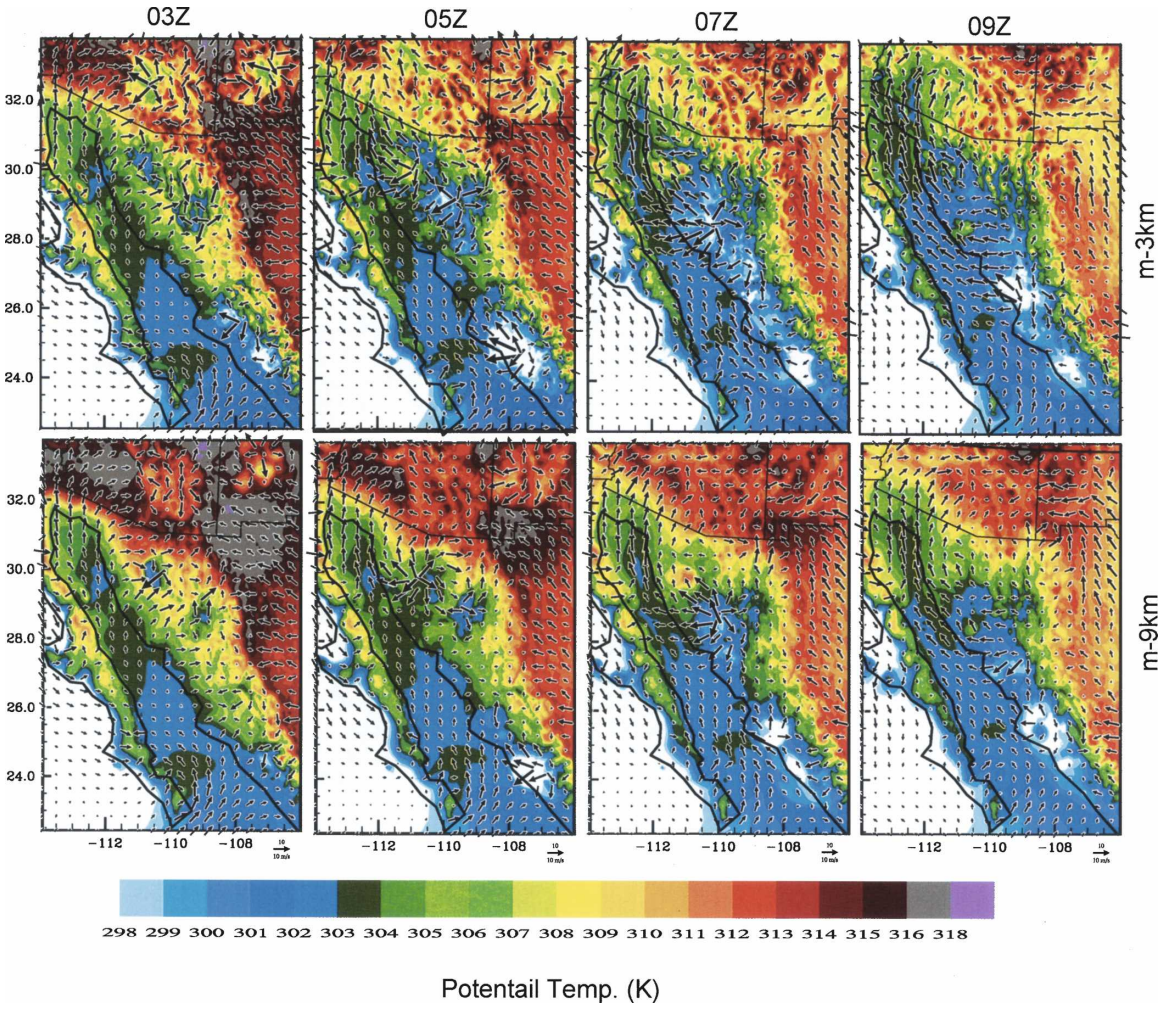

FIG. 13. The wind vector and potential temperature at 29 sigma levels at 0300, 0500, 0700, and 0900 UTC 13 Jul 2004.

case 1, the LLJ over the northern Gulf of California and the convection over northwestern Mexico are relatively weak. Thus, it is reasonable to conclude that the convection over northwestern Mexico can modulate the intensity of the LLJ over the northern GOC.

Also worthy of mention is that unlike the surge case, the model is not capable of generating rainfall in the second day. For example, on 12 August the radar shows there was strong convection along the SMO from the late afternoon, while the model generated very weak convection over the southern part of the SMO (figure not shown). This result indicates that the forcing data are very important in the current mesoscale model.

TABLE 1. Low-level southerly wind (m s^{-1}) comparisons between models and ISS4 observation at 0600 UTC 13 Jul 2004.

	Observation	9-km resolution model	3-km resolution model
950 mb	11	4	12
975 mb	9	5	13
1000 mb	7	4	12

3) LIMITED TEST RESULTS FOR 1-KM RESOLUTION

By checking the radar data from 0100 to 0500 UTC 10 July 2004, we noticed that there was an isolated convective system, which was located between ~24° and 26°N and between ~108° and 106°W, with a rain rate of ~5–10 mm h^{-1}. Both the 3- and 9-km model runs missed this storm.

To examine whether increasing the resolution can capture the storm, we nested a 1-km resolution domain in domain 3 and reran the model. The 1-km model still could not capture the storm (not shown). We also tried to use 1-km resolution to see if the nighttime storm,

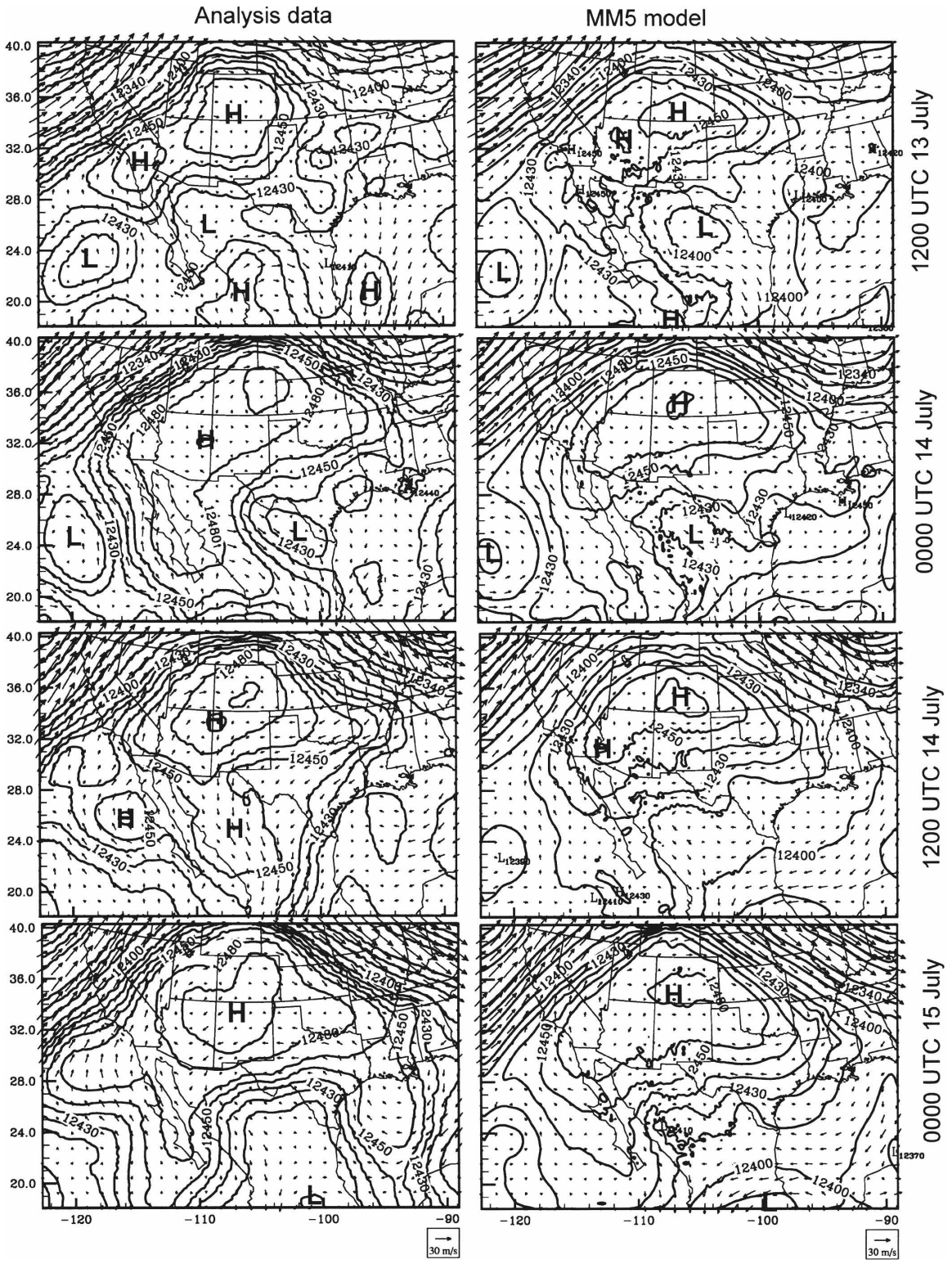

FIG. 14. 200-mb heights (m) and wind vector (m s^{-1}) from Eta Model analysis and MM5 domain 1 output. High and low heights are labeled with H and L, respectively. The height contours have 30-m intervals when heights are less than 12 400 m, while 20-m intervals are used when heights are greater than 12 400 m.

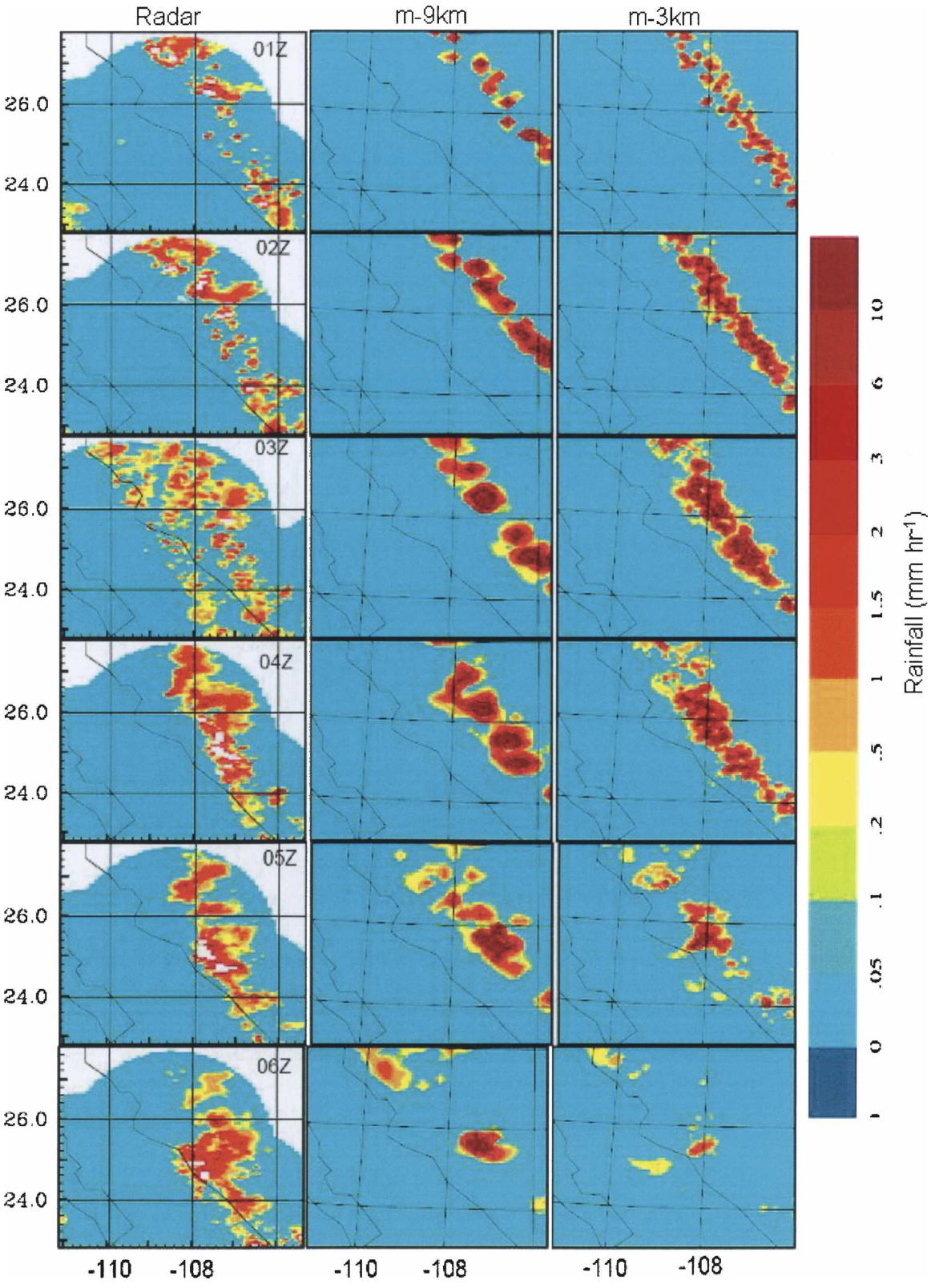

FIG. 15. The rainfall-rate comparison between radar data and model results from 0100 to 0600 UTC 13 Aug 2004.

which occurred in 13 July, could be captured by the model. Even at this resolution, the model still could not simulate the rainfall in comparison with the observation (not shown). These two sensitivity tests indicate that the model at current configurations and forcing data have deficiencies in simulating the convective storms over the west slope of the SMO at nighttime and the coastal low-elevation areas.

4. Conclusions

A major NAME tier I research question concerns the effect of increased resolution on the fidelity of convective rainfall processes. In this study we partly addressed this question using different spatial resolutions (9 and 3 km) and a mesoscale model (MM5). A summary of key results is as follows:

1) The model captures some of the mean characteristics of the diurnal cycle of precipitation. In general, rainfall begins too early in the model at high elevations. The model is unable to capture details of the diurnal cycle even at high resolution. In particular, the model reproduces neither the rainfall over the GOC nor the nighttime rainfall at lower elevations along the coast of the GOC and along the west slopes of the SMO, in part because of the model's inability to simulate the vertical structure of meteorological fields.
2) At a higher resolution the modeled diurnal cycle of rainfall is improved in amount and intensity when compared to the NERN data. At coarse resolution the model generates unrealistically high amounts (>20 mm) over the hills along the SMO.
3) Increasing resolution does not improve the simulation of the nighttime GOC LLJ or the low-level surface winds over the GOC; in general, the modeled winds are too weak.
4) Case studies from the model indicate that the convective outflows from the western slope of the SMO, especially from northwestern Mexico, can modulate the intensity of the GOC LLJ. Case studies and sensitivity studies also indicate that the initial and boundary conditions (forcing fields) are important in predicting the rainfall variability.

Overall, we conclude that the higher-resolution model performs better over mountainous areas. At the same time, there was little difference (if any) between the two resolutions over the Gulf of California and the lower-elevation coastal areas. These results imply that to quantitatively forecast the rainfall over western Mexico and the southwestern United States, the model's ability to describe the vertical structure of meteorological fields, as well as forcing fields, needs to be improved.

Acknowledgments. The authors are grateful to the reviewers for their welcome and constructive suggestions. Primary support for this research was provided by the NASA NEWS program (NNG06GB20G), the NOAA GAPP Program (NA16GP1605), and the NSF STC Program (Agreement EAR-9876800). The first author thanks Drs. Jimmy M. Ferng and Kathleen Bowles, and other staff at the Computer Center and Information Technology, University of Arizona, for their help and support.

REFERENCES

Adams, D. K., and A. C. Comrie, 1997: The North American monsoon. *Bull. Amer. Meteor. Soc.,* **78,** 2197–2213.

Anderson, B. T., J. O. Roads, S.-C. Chen, and H.-M. H. Juang, 2001: Model dynamics of summertime low-level jets over northwestern Mexico. *J. Geophys. Res.,* **106** (D4), 1–13.

Barlow, M., S. Nigam, and E. H. Berbery, 1998: Evolution of the North American monsoon system. *J. Climate,* **11,** 2238–2257.

Berbery, E. H., 2001: Mesoscale moisture analysis of the North American monsoon. *J. Climate,* **14,** 121–137.

Chen, F., and J. Dudhia, 2001: Coupling an advanced land surface–hydrology model with the Penn State–NCAR MM5 modeling system. Part I: Model implementation and sensitivity. *Mon. Wea. Rev.,* **129,** 569–585.

Ciesielski, P. E., and R. H. Johnson, 2008: Diurnal cycle of surface flows during 2004 NAME and comparison to model reanalysis. *J. Climate,* **21,** 3890–3913.

Douglas, M. W., and S. Li, 1996: Diurnal variation of the lower-tropospheric flow over the Arizona desert from SWAMP-93 observation. *Mon. Wea. Rev.,* **124,** 1211–1224.

——, R. A. Maddox, K. Howard, and S. Reyes, 1993: The Mexican monsoon. *J. Climate,* **5,** 1665–1677.

——, A. Valdez-Manzanila, and R. G. Cueta, 1998: Diurnal variation and horizontal extent of the low-level jet over the northern Gulf of California. *Mon. Wea. Rev.,* **126,** 2017–2025.

Fawcett, P. J., J. R. Stalker, and D. S. Gutzler, 2002: Multistage moisture transport into the interior of northern Mexico during the North American summer monsoon. *Geophys. Res. Lett.,* **29,** 2094, doi:10.1029/2002GL015693.

Gao, X., J. Li, and S. Sorooshian, 2007: Modeling intraseasonal features of 2004 North American monsoon precipitation. *J. Climate,* **20,** 1882–1896.

Garreaud, R. D., and J. M. Wallace, 1997: The diurnal march of convective cloudiness over the Americas. *Mon. Wea. Rev.,* **125,** 3157–3171.

Gebremichael, M. E., R. Vivoni, C. J. Watts, and J. C. Rodriguez, 2007: Submesoscale spatiotemporal variability of North American monsoon rainfall over complex terrain. *J. Climate,* **20,** 1751–1773.

Gochis, D. J., W. J. Shuttleworth, and Z.-L. Yang, 2002: Sensitivity of the modeled North American monsoon regional climate to convective parameterization. *Mon. Wea. Rev.,* **130,** 1282–1298.

——, A. Jimenez, C. J. Watts, J. Garatuza-Payan, and W. J. Shuttleworth, 2004: Analysis of 2002 and 2003 warm-season precipitation from the North American Monsoon Experi-

ment event rainfall gauge network. *Mon. Wea. Rev.,* **132,** 2938–2953.

——, C. J. Watts, J. Garatuza-Payan, and J. Cesar-Rodriguez, 2007: Spatial and temporal patterns of precipitation intensity as observed by the NAME event rain gauge network from 2002 to 2004. *J. Climate,* **20,** 1734–1750.

Grell, G. A., 1993: Prognostic evaluation of assumptions used by cumulus parameterizations. *Mon. Wea. Rev.,* **121,** 764–787.

Higgins, R. W., Y. Yao, and X. L. Wang, 1997: Influence of the North American monsoon system on the U.S. summer precipitation regime. *J. Climate,* **10,** 2600–2622.

——, Y. Chen, and A. V. Douglas, 1999: Interannual variability of the North American warm season precipitation regions. *J. Climate,* **12,** 653–680.

——, and Coauthors, 2006: The NAME 2004 field campaign and modeling strategy. *Bull. Amer. Meteor. Soc.,* **87,** 79–94.

Higgins, W., and D. Gochis, 2007: Synthesis of results from the North American Monsoon Experiment (NAME). *J. Climate,* **20,** 1601–1607.

Hong, S.-Y., and H.-L. Pan, 1996: Nonlocal boundary layer vertical diffusion in a medium-range forecast model. *Mon. Wea. Rev.,* **124,** 2322–2339.

Johnson, R., P. Ciesielski, B. McNoldy, P. Rogers, and R. Taft, 2007: Multiscale variability of the flow during the North American monsoon experiment. *J. Climate,* **20,** 1628–1647.

Lang, T., D. Ahijrvych, S. Nesbitt, R. Carbone, S. Rutledge, and R. Cifelli, 2007: Radar-observed characteristics of precipitating system during NAME 2004. *J. Climate,* **20,** 1713–1733.

Li, J., X. Gao, R. A. Maddox, and S. Sorooshian, 2004: Model study of evolution and diurnal variation of rainfall in the North American monsoon during June and July 2002. *Mon. Wea. Rev.,* **132,** 2895–2915.

Luo, H., and M. Yanai, 1983: The large-scale circulation and heat sources over the Tibetan Plateau and surrounding areas during the early summer of 1979. Part I: Precipitation and kinematic analysis. *Mon. Wea. Rev.,* **111,** 922–944.

Mesinger, F., and Coauthors, 2006: North American Regional Reanalysis. *Bull. Amer. Meteor. Soc.,* **87,** 343–359.

Mo, K. C., and H. M. H. Juang, 2003: Influences of sea surface temperature anomalies in the Gulf of California on North American monsoon rainfall. *J. Geophys. Res.,* **108,** 4112, doi:10.1029/2002JD002403.

——, J. Schemm, H. M. H. Juang, R. W. Higgins, and Y. Song, 2005: Impact of model resolution on the prediction of summer precipitation over the United States and Mexico. *J. Climate,* **18,** 3910–3927.

Negri, A., R. Adler, R. Maddox, K. Howard, and P. Keehn, 1993: A regional rainfall climatology over Mexico and southwest United States derived from passive microwave and geosynchronous infrared data. *J. Climate,* **6,** 2144–2161.

——, ——, and G. Guffman, 1994: Regional rainfall climatologies derived from Special Sensor Microwave Imager (SSM/I) data. *Bull. Amer. Meteor. Soc.,* **75,** 1165–1182.

Saleeby, S. M., and W. R. Cotton, 2004: Simulations of the North American Monsoon system. Part I: Model analysis of the 1993 monsoon system. *J. Climate,* **17,** 1997–2018.

Sorooshian, S., X. Gao, K. Hsu, R. A. Maddox, Y. Hong, H. V. Gupta, and B. Iman, 2002: Diurnal variability of tropical rainfall retrieved from combined GOES and TRMM satellite information. *J. Climate,* **15,** 983–1001.

Stensrud, D. J., R. L. Gall, S. L. Mullen, and K. W. Howard, 1995: Model climatology of the Mexican monsoon. *J. Climate,* **8,** 1775–1794.

——, ——, and M. K. Nordquist, 1997: Surges over the Gulf of California during the Mexican monsoon. *Mon. Wea. Rev.,* **125,** 417–437.

Tao, W.-K., and J. Simpson, 1989: Modeling of a tropical squall-type convective line. *J. Atmos. Sci.,* **46,** 177–202.

Vivoni, E. R., and Coauthors, 2007: Variation of hydrometeorological conditions along a topographic transect in northwestern Mexico during the North American monsoon. *J. Climate,* **20,** 1792–1809.